Organic Electronics 13 (2012) 394–398

Contents lists available at SciVerse ScienceDirect

Organic Electronics

journal homepage: www.elsevier.com/locate/orgel

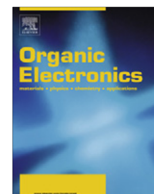

# Dependence of charge carrier mobility of 4,4′,4″-tris (N-3-methylphenyl-N-phenylamino)triphenylamine on doping concentration of tetrafluoro-tetracyano-quinodimethane

Gayatri Chauhan [a,b], Ritu Srivastava [a,*], Arunandan Kumar [a], Omwati Rana [a], P.C. Srivastava [b], M.N. Kamalasanan [a]

[a] Center for Organic Electronics, National Physical Laboratory (Council of Scientific & Industrial Research), Dr. K.S. Krishnan Road, New Delhi 110012, India
[b] Department of Physics, Banaras Hindu University, Varanasi 221005, India

ARTICLE INFO

*Article history:*
Received 30 March 2011
Received in revised form 23 September 2011
Accepted 21 November 2011
Available online 19 December 2011

*Keywords:*
Doping
Injection efficiency
SCLC

ABSTRACT

Electrical transport of pure and tetrafluoro-tetracyano-quinodimethane doped 4,4′,4″-tris(N-3-methylphenyl-N-phenylamino)triphenylamine (m-MTDATA) films have been studied at various temperatures and doping concentrations. Pure films show space charge limited conduction with field and temperature dependent mobility. The *J–V* characteristics of doped m-MTDATA were ohmic at low voltages due to thermally released carriers from dopant states. At higher voltages the current density increases nonlinearly due to field dependent mobility and carrier concentration thereby filling of tail states of HOMO of the host. The conductivity of doped films were analysed using the Unified Gaussian Disorder Model (UGDM). The carrier concentration obtained from the fitting show a non-linear dependence on doping concentration which may be due to a combined effect of thermally activated carrier generation and increased carrier mobility.

© 2011 Elsevier B.V. All rights reserved.

## 1. Introduction

Electrical doping of organic semiconductors is one of the most important areas of organic semiconductor research at present and many researchers are engaged in understanding the fundamental aspects of this issue [1,2]. Electrical doping is usually done to reduce the electrical resistance of the electron and hole transport layers in organic devices. Electron transport layers are usually doped n-type and hole transport layers are doped p-type. The usual dopants used for p-type doping are strong acceptors like tetrafluoro-tetracyano-quinodimethane ($F_4$-TCNQ), where as for n-type doping low work function metals and related compounds are used [3,4]. Doping usually creates shallow trapping levels and moves the Fermi level of the semiconductor towards the transport states. The reduction in electrical resistivity upon doping is well documented [5,6]. It has been suggested by many authors that electrical doping fills up the tail states of Gaussian distributed transport states and enhances the charge carrier mobility [7]. Very little experimental evidences are available in this regard. We have doped the hole transport material 4,4′,4″-tris(N-3-methylphenyl-N-phenylamino) triphenylamine (m-MTDATA) with an acceptor $F_4$-TCNQ and studied its effect on the transport properties of the host material and the results obtained are reported in this letter.

## 2. Experimental

Hole only samples of m-MTDATA films were prepared in the configuration ITO/m-MTDATA (300 nm)/Au. 1 nm of pure $F_4$-TCNQ was inserted in between the electrodes and m-MTDATA films for making ohmic contact. 120 nm ITO sputtered on glass plates (Vin Karola, USA) were patterned and solution cleaned ultrasonically and treated

* Corresponding author. Tel.: +91 1145608596.
*E-mail address:* ritu@mail.nplindia.org (R. Srivastava).

1566-1199/$ - see front matter © 2011 Elsevier B.V. All rights reserved.
doi:10.1016/j.orgel.2011.11.023

with oxygen plasma were used as substrates. Gold and organic materials were thermally vacuum evaporated onto the substrates and the doping was done by co-evaporation. Electrical measurements were done using Keithley 2610 source measure unit interfaced with computer. All measurements were done in a cryostat (Advanced Research systems Inc., USA) in vacuum conditions. The *J–V* characteristics of m-MTDATA were measured in the configuration ITO/m-MTDATA/Au.

## 3. Results and discussion

Before analyzing any results on charge transport it is necessary to confirm that the electrical contacts of the injecting electrodes are ohmic or not by calculating the injection efficiency of the contacts. Even though some earlier reports [8,9] suggests ohmic contact in case of ITO/m-MTDATA interface, the value of hole mobility reported by them from *J–V* measurements is substantially different from those obtained by TOF measurements. Therefore to confirm the hole injection property ITO/m-MTDATA interface the measured current density $J_{obs}$ has been compared with the current density expected from trap free space charge limited conduction $J_{SCLC}$ [10]. The injection efficiency ($\eta$) is given as

$$\eta = J_{obs}/J_{SCLC}.$$

The injection efficiency will be 1 for pure ohmic contact. The value of $J_{SCLC}$ is calculated by using the Murgatroyd equation [11]

$$J(F,T) = \frac{9}{8}\varepsilon\varepsilon_0\frac{V^2}{d^3}\mu_h(0,T)\exp(0.89\gamma\sqrt{F}) \quad (1)$$

where $\varepsilon$ is the dielectric constant taken as 3 for m-MTDATA, $\varepsilon_0$ is the permittivity of free space, $\mu_h(0,T)$, the temperature dependent zero field mobility of holes, $d$ the thickness of the film and $F = V/d$ is the electric field.

In the present case, the injection efficiency of ITO/m-MTDATA/Au calculated at 3 V at room temperature by Eq. (1) taking zero field mobility value from time of flight (TOF) experiments [12] ($\mu_0 = 1.3 \times 10^{-5}$ cm$^2$/V s, $\gamma = 2.0 \times 10^{-3}$ (V/cm)$^{-1/2}$) was 0.08. Therefore to study the bulk properties of m-MTDATA, it was found necessary to modify the interface and thereby the charge injection properties. Based on the Fermi-level alignment property of metals with polaronic states of $F_4$-TCNQ and subsequent enhancement of substrate work function [13], we have inserted ultra thin films (1 nm) of thermally evaporated pure $F_4$-TCNQ between the electrodes ITO, Au and m-MTDATA films. After the addition of the interface layer, the injection efficiency has increased near to unity for all applied voltages (Fig. 1). Further, the current in the forward and reverse directions were also similar (inset of Fig. 1) indicating negligible built-in potential in the samples. Therefore for all further studies, the interfacial layer has been inserted between the electrodes and m-MTDATA to ensure ohmic contact.

Fig. 2(a) shows the *J–V* characteristics of the interface modified ITO/$F_4$-TCNQ/m-MTDATA (300 nm)/$F_4$-TCNQ/Au structure in log–log scale at temperatures 300, 273, 247, 222, 194 and 163 K. At room temperature and low electric

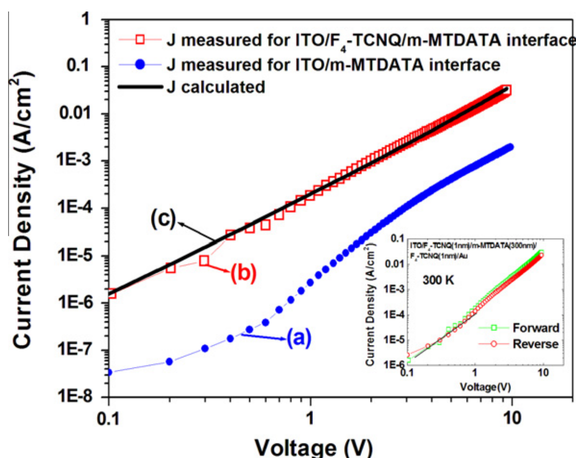


**Fig. 1.** *J–V* characteristics of (a) ITO/m-MTDATA (300 nm)/Au (b) ITO/$F_4$-TCNQ (1 nm)/m-MTDATA (300 nm)/$F_4$-TCNQ (1 nm)/Au and (c) calculated for SCLC using Murgatroyd equation. Inset: Current density in the forward and reverse direction for interface modified device.

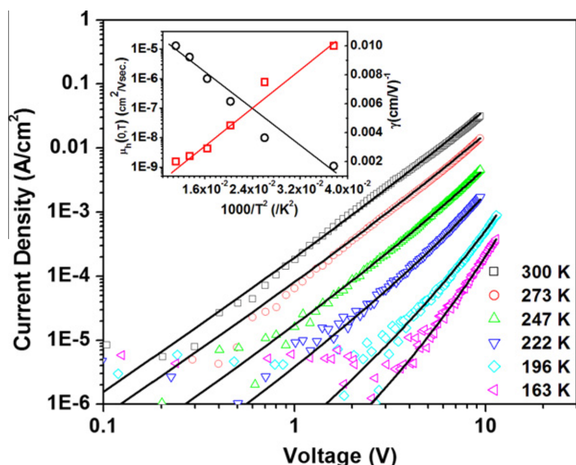


**Fig. 2a.** *J–V* characteristics of 300 nm thick m-MTDATA hole-only samples at 300, 273, 247, 222, 196 and 163 K. Inset shows the variation of zero filed mobility ($\mu_0$) and $\gamma$ with 1000/$T^2$.

fields, the *J–V* characteristics show a slope of 2 indicating SCLC. To confirm SCLC in m-MTDATA films with modified electrodes, the thickness dependence of *J* in these films has been studied at room temperature and shown in Fig. 2(b). In pure films at low voltages, the field dependence of *J* with electric field is low and the current density show square law dependence with voltage. In this region the current density scale with $1/d^3$ in SCLC and a plot of *J* vs. $1/d^3$ should show a straight line. Inset of Fig. 2(b) shows the variation of current density for voltages 0.3, 0.7 and 1 V with the inverse of the cube root of thickness ($d$) 100, 200 and 300 nm respectively at 300 K. The plot shows straight line behaviour suggesting a space charge limited conduction mechanism. The *J–V* characteristic deviates from the slope of 2 as the voltage increased (Fig. 2(a)). Further, as the temperature is decreased, it shows substantial decrease in current density at low bias voltages. These observations suggest a field

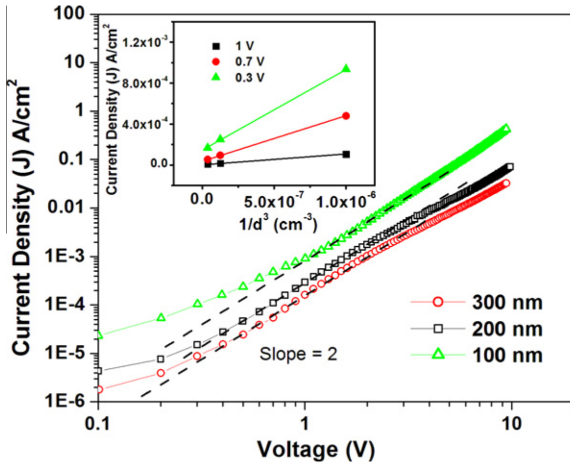


**Fig. 2b.** $J$–$V$ characteristics of 100, 200 and 300 nm thick m-MTDATA hole-only samples. The dashed line shows the slope of 2. Inset shows the variation of $J$ with $1/d^3$.

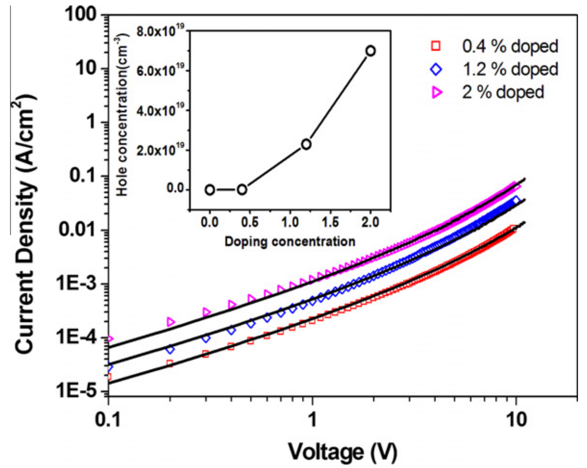


**Fig. 3a.** $J$–$V$ characteristics of 300 nm thick 0.4, 1.2 and 2 wt% $F_4$-TCNQ doped m-MTDATA hole-only samples at room temperature. The solid lines are simulated curves. Inset shows the variation of conductivity at different doping concentration of $F_4$-TCNQ in m-MTDATA.

and temperature dependent charge carrier mobility. The current density simulated using Eq. (1) (continuous line in Fig. 2(a)) shows that the observed values of $J$ fits very well with the simulated values calculated using values of $\mu_0(T)$ and $\gamma$ for each temperature. The value of zero field mobility obtained from the present analysis at room temperature is $1.3 \times 10^{-5}$ cm$^2$/V s and is very near to the value reported from TOF measurements [12]. The estimated value of zero field mobility $\mu_0(T)$ and field dependent factor $\gamma$ has been analyzed on the basis of Gaussian disorder model which leads to the following form of mobility

$$\mu(F,T) = \mu_\infty \exp\left(-\left(\frac{2}{3}\hat{\sigma}\right)^2\right) \exp(C\{(\hat{\sigma})^2 - \Sigma^2\}\sqrt{F}) \qquad (2)$$

where $\hat{\sigma} = \frac{\sigma}{k_b T}$, $\Sigma$, $C$ and $\mu_\infty$ are the energetic disorder, positional disorder, specific parameter and high temperature limit of mobility respectively. The zero field mobility $\mu(0,T)$ and $\gamma(T)$ can be expressed as

$$\left.\begin{array}{l} \mu(0,T) = \mu_\infty \exp\left(-\left(\frac{2}{3}\hat{\sigma}\right)^2\right) \\ \gamma(T) = C\{(\hat{\sigma})^2 - \Sigma^2\} \end{array}\right\} \qquad (3)$$

In the inset of Fig. 2(a), the fitted values of zero field mobility as well as the field dependent factor $\gamma$ are also plotted against $1000/T^2$. The zero field mobility of charge carriers decrease with decrease in temperature the log of which shows linear dependence on $1000/T^2$ whereas the field depend factor $\gamma$ increases with decrease in temperature, again showing a dependence of $1000/T^2$. From the present analysis the value of $\sigma$ = 78 meV, $\Sigma$ = 4.6, $\mu = 4.54 \times 10^{-4}$ cm$^2$/V s and $C = 3.9 \times 10^{-4}$ (cm/V)$^{1/2}$ have been obtained.

To find out the effect of $F_4$-TCNQ doping on m-MTDATA, we have studied the $J$–$V$ characteristics of this material with doping concentrations of 0.4, 1.2 and 2 wt% of the dopant $F_4$-TCNQ in m-MTDATA at room temperature as shown in Fig. 3(a). Pure m-MTDATA starts with a slope of 2 which slowly increase with increase in applied voltage

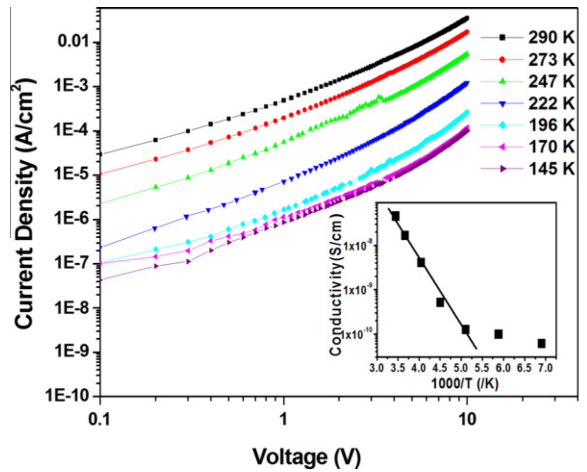


**Fig. 3b.** $J$–$V$ characteristics of 300 nm thick 1.2% $F_4$-TCNQ doped m-MTDATA hole-only samples at different temperature. Inset shows the conductivity vs. $1000/T$ plot of 1.2% $F_4$-TCNQ doped m-MTDATA at 0.4 V.

where as for the doped samples at low voltages, $J$–$V$ characteristics show a slope of 1 showing ohmic conduction and $J$ at constant voltage increases with increase in doping concentration. The value of the conductivity ($\sigma$) was calculated from this region and shown in inset of Fig. 3(b).

At higher electric field the current density of doped layers was fitted using the Unified Gaussian Disorder Model [14] taking into account the dependence of charge carrier mobility with temperature, carrier density and electric field. According to this model

$$J = p(x)e\mu(T, p(x), E(x))E(x) \qquad (4)$$

where $x$ is the distance from the injecting electrode and

$$\mu_p(T,p,E) \approx \mu_0(T,p)f(T,E) \qquad (5)$$

with

$$\mu_0(T,p) = \mu_0(T)\exp\left[\frac{1}{2}(\hat{\sigma}^2 - \hat{\sigma})(2pa^3)^{\delta}\right]$$

where

$$\mu_0(T) = \mu_0 c_1 \exp(-c_2\hat{\sigma}^2)$$

$$\delta = 2\frac{\ln(\hat{\sigma}^2 - \hat{\sigma}) - \ln(\ln 4)}{\hat{\sigma}^2}$$

$$\mu_0 = \frac{a^2 v_0 e}{\sigma}$$

and

$$f(T,E) = \exp\left\{0.44(\hat{\sigma}^{3/2} - 0.22)\left[\sqrt{1 + 0.8\left(\frac{Eea}{\sigma}\right)^2} - 1\right]\right\}$$

where $\hat{\sigma} \equiv \frac{\sigma}{K_bT}$ with $\sigma$ the width of the Gaussian DOS, $a = 1.2$ nm, is the lattice constant, $v_0 = 2.8 \times 10^{11}$, is an intrinsic rate, $\mu_p$ the hole mobility and $p = p_0\ \exp(\gamma\sqrt{E})$ where $p_0$ is the hole density and $\gamma$ is filed lowering factor [15]. From which the value of energetic disorder has been obtained as $\sigma = 72$ meV for pure m-MTDATA and 80 meV for doped m-MTDATA.

Fig. 3(a) shows the *J–V* characteristics observed and that fitted using Eqs. (4) and (5) from where the charge density due to electrical doping has been evaluated. The experimental results represented by open symbols fit very well with the *J–V* characteristics calculated using Eqs. (4) and (5) (black solid line). The values of hole density and obtained from the fitting has been plotted against doping concentration and shown in inset of Fig. 3(a) which shows nonlinear relation with doping concentration. The charge carrier concentration of the films increases with doping concentration and applied field. Fig. 3(b) shows the *J–V* characteristics of ITO/$F_4$-TCNQ/1.2 wt% $F_4$-TCNQ doped m-MTDATA (300 nm)/$F_4$-TCNQ/Au samples at temperatures 290, 273, 247, 222, 196, 170, 145 and 120 K. At low bias voltages, the curves show ohmic conduction whereas at higher voltages, the curves show a non-linear dependence of current on voltage indicating a ohmic conduction with field dependent carrier concentration. The nonlinear behaviour of *J–V* characteristics at high voltage is a result of field dependent mobility and field assisted release of holes from the dopants. In the inset of Fig. 3(b), the log of conductivity of the sample at 0.4 V is plotted against 1000/*T* which gives a straight line showing Arrhenius dependence on temperature. From the slope of this graph the value of activation energy was calculated as 0.15 eV.

From the above observations the following results can be summarized.

1. Pure ITO/m-MTDATA interface is not perfectly ohmic. The modification of its interface with an ultra thin layer of $F_4$-TCNQ provides ohmic contact.
2. ITO/$F_4$-TCNQ/m-MTDATA/$F_4$-TCNQ/Au samples are showing SCLC conduction with field and temperature dependent charge carrier mobility.
3. During the electrical doping of $F_4$-TCNQ into m-MTDATA, the low field conduction is controlled by thermally activated carrier generation as well as enhanced mobility due to doping. High field conduction is controlled by field dependent mobility and carrier concentration.
4. The hole conductivity has increased non-linearly with doping concentration.

Pure m-MTDATA is a good insulator and have only very few intrinsic free carriers. Therefore even at low injection of holes into this material produce space charge and the charge transport is controlled by SCLC. As observed in many organic semiconductors the charge carrier mobility is influenced by temperature and electric field [16]. When strong acceptors like $F_4$-TCNQ is introduced into the semiconductor, acceptor states are created near the HOMO of the semiconductor and its Fermi level moves towards the acceptor levels and charge carriers are thermally generated. It is well documented [17,18] that the doping of $F_4$-TCNQ into organic semiconductors like zinc phthalocyanine (ZnPc) and *N*,*N*′-di-[(1-naphthalenyl)-*N*,*N*′-diphenyl]-(1.1′biphenyl)-4,4′-diamine (α-NPD) brings the Fermi level towards the HOMO of the organic semiconductor indicating that acceptor levels are created near the HOMO of the organic semiconductor. These acceptor states are neutral when empty and charged when filled by an electron. In the doping process, these acceptor states trap electrons from the bulk of the host and make them more p-type. The trapping process is governed by thermodynamics and the charge carriers from the dopant to the HOMO of the host material will be a thermally activated process.

At low doping concentrations the free carriers generated from the ionization of the dopants will be higher than the background doping and hence the thermally activated charge carriers from the dopant will be the main contributor of free carriers. In this case the conductivity follows the Arrhenius nature. This explains our observation (inset of Fig. 3(b)) where the $\log\sigma$ against 1000/*T* gives a straight line with an activation energy of 0.15 eV. As the doping concentration increases more carriers will be released from the dopants and the Fermi level moves more towards the trap states. This causes charge transport to occur at higher energy levels where the density of states and consequently the hopping rate for charge transport is higher resulting in increase in charge carrier mobility (percolation model) [7]. The results were analyzed on the basis of the Unified GDS Model [14].

The doping of the organic semiconductor has increased the disorder in the material [19,20] as evidenced by an increase in disorder ($\sigma$) from 72 meV for pure films to 80 meV in doped samples. As the doping concentration is increased, carriers released from the dopant increases. This together with the effect of the increase in charge carrier mobility is a probable reason for the non-linear dependence of the conductivity on doping concentration observed at low voltages.

## 4. Conclusions

In conclusion, we have studied the doping effect on the charge carrier generation and mobility of m-MTDATA. We

found that the doping increases the free carrier density as well as charge carrier mobility in the semiconductor. These free carriers are thermally generated from the acceptor states. The combined effect of the increase in free carrier density and the increase in charge carrier mobility is the reason for the non-linear nature of conductivity with doping observed at low electric fields.

## Acknowledgements

The authors are thankful to CSIR (India) for financial assistance.

## References

[1] U. Bach, D. Lupo, P. Comte, J.E. Moser, F. Weissörtel, J. Salbeck, H. Spreitzer, M. Grätzel, Nature 395 (1998) 583.
[2] K. Walzer, B. Maennig, M. Pfeiffer, K. Leo, Chem. Rev. 107 (2007) 1233.
[3] X. Zhou, J. Blochwitz, M. Pfeiffer, A. Nollau, T. Fritz, K. Leo, Adv. Funct. Mater. 11 (2001) 310.
[4] T. Matsushima, C. Adachi, Appl. Phys. Lett. 89 (2006) 253506.
[5] J. Hwang, A. Kahn, J. Appl. Phys. 97 (2005) 103705.
[6] Y. Shen, K. Diest, M.H. Wong, B.R. Hsieh, D.H. Dunlap, G.G. Malliaras, Phys. Rev. B 68 (2003) 081204R.
[7] B. Maennig, M. Pfeiffer, A. Nallau, X. Zhou, K. Leo, P. Simon, Phys. Rev. B 64 (2001) 195208.
[8] Toshinori Matsushima, Guang-He Jin, Yoshihiro Kanai, Tomoyuki Yokota, Seiki Kitada, Toshiyuki Kishi, Hideyuki Murata, Org. Electron. 12 (2011) 520.
[9] Carsten Giebelera, Homer Antoniadis, Donal D.C. Bradley, Yasuhiko Shirota, Appl. Phys. Lett. 72 (1998) 2448.
[10] A.J. Campbell, D.D.C. Bradley, H. Antoniadis, J. Appl. Phys. 89 (2001) 3343.
[11] P.N. Murgatroyd, J. Phys. D 3 (1970) 151.
[12] S.W. Tsang, S.K. So, J.B. Xu, J. Appl. Phys. 99 (2006) 013706.
[13] S. Braun, W.R. Salaneck, Chem. Phys. Lett. 438 (2007) 259.
[14] W.F. Pasveer, J. Cottaar, C. Tanase, R. Coehoorn, P.A. Bobbert, P.W.M. Blom, D.M. DeLeeuw, M.A.J. Michels, Phys. Rev. Lett. 94 (2005) 206601.
[15] Y. Zhang, P.W.M. Blom, Org. Electron. 11 (2010) 1261.
[16] H. Bassler, Phys. Stat. Sol. (b) 175 (1993) 15.
[17] J. Blochwitz, T. Fritz, M. Pfeiffer, K. Leo, D.M. Alloway, P.A. Lee, N.R. Armstrong, Org. Electron. 2 (2001) 297.
[18] W. Gao, A. Kahn, J. Appl. Phys. 94 (2003) 359.
[19] V.I. Arkhipov, P. Heremans, E.V. Emelianova, H. Bässler, Phys. Rev. B 71 (2005) 045214.
[20] D. Poplavskyy, J. Nelson, J. Appl. Phys. 93 (2003) 341.